Available online at www.sciencedirect.com

SciVerse ScienceDirect

Energy Procedia 37 (2013) 2341 – 2348

Energy Procedia

GHGT-11

Fundamental modeling of a membrane reactor with in situ hydrogen separation and combustion

Torleif Weydahl[a], Prashant Salimath[b], Andrea Gruber[a]*

[a]*SINTEF Energy Research, Pb. 4761 Sluppen, NO-7465 Trondheim, Norway*
[b]*Norwegian Universtiy of Science and Technology, Dep. Energy and Process Engineering, …*

Abstract

In this work we consider a membrane reactor with catalytic steam methane reforming and/or water gas shift on the feed side, hydrogen separation and direct combustion of hydrogen on the permeate side, where the ultimate goal is an industrial size novel integrated membrane reactor/combustor concept. The concept has a potential of increasing the efficiency of pre-combustion carbon capture power plants. The present work focuses on the fundamental properties of membrane-flame interaction, which is of relevance to the membrane-combustor concept. A model has been implemented into a high-order finite differences direct numerical simulation code (S3D), which takes into account that a single species (hydrogen in this case) is transported through a permeable wall by the partial pressure difference between the feed and the permeate side. The model enables detailed simulation of membrane-flame interaction on the permeate side in 3-dimensional geometries. Preliminary results indicate that the flame thickness at quenching decreases when the permeable wall is present. This may be due to the enrichment of the zone close to the wall caused by the hydrogen flux. Small differences are also found for the quenching time and the quenching distance.

Selection and/or peer-review under responsibility of GHGT

Keywords: Pre-combustion CCS; H_2 membrane;flame-wall interaction; flame quenching

1. Introduction

Large scale implementation of CO_2 Capture and Storage (CCS) technologies is prevented by the high cost on CCS being e.g. two to four times the present European trading cost on CO_2 emissions [1]. Considering the pre-combustion CCS option from stationary gas power production, a significant part of the energy and efficiency penalty, i.e. the added cost, is related to the reforming and separation of hydrogen from the natural gas [2]. Present technology concepts use Auto-Thermal Reforming (ATR) or Steam Methane Reforming (SMR) with Water Gas Shift (WGS) reactors to produce the H_2-rich syngas

* Corresponding author. Tel.: +47 735 93699
E-mail address: andrea.gruber@sintef.no

1876-6102
Selection and/or peer-review under responsibility of GHGT
doi:10.1016/j.egypro.2013.06.115

from natural gas, while CO_2 is separated from the syngas by adsorption [3]. One potentially more efficient alternative is to introduce a hydrogen catalytic membrane where the reforming, the water gas shift and the H_2 separation from CO_2 are combined in the same unit [4]. For stationary coal power production with Integrated Gasification Combined Cycle (IGCC), a membrane reactor may replace the WGS and the CO_2 separation unit [5]. The reforming and/or water gas shift reactions on the feed side are enhanced by the continuous removal of hydrogen on the permeate side [6].

In this work we consider a membrane reactor with catalytic SMR and/or WSG on the feed side, hydrogen separation and direct combustion of hydrogen on the permeate side. The ultimate goal is an industrial size novel membrane reactor/combustor concept, hence, large flow rates are needed and the sweep-gas flow may become turbulent at given conditions. The present work is based on a simulation model which is three-dimensional in general, and a modeling approach which does not make any pre-assumptions on whether the flow is laminar or turbulent. Palladium (Pd) membranes are operating in the range 300-400°C with high flux of hydrogen, while ceramic membranes are best operating around 800-1000°C, however, the hydrogen flux of the latter is relatively low. The selection of the optimal type of membrane will be one of the final outcomes of the modeling work initiated with the present paper.

The aim of the present study is to gain insight into the fundamental phenomena of flame stabilization and blow-off when the hydrogen fuel is supplied through a permeable wall to the oxidizer on the feed side. As a first approach, the basic properties regarding flame quenching towards a permeable wall is studied in detail using a one-dimensional approach, based on a direct numerical simulation (DNS) code. In its complete 3-D form, DNS makes no assumptions on flow regimes [8]; the effect of turbulent transport and molecular mixing is not modeled, but rather resolved in 3-D on the computational grid. DNS has been used for two decades to study unconfined turbulent flames with unprecedented level of detail and only recently has been applied to study flame-wall interaction processes [9].

Several numerical investigations of flame wall quenching exist in the literature for methane [10]. The quenching Peclet number, defined later in section 3.2, is typically reported to be in the range of 3.0 for methane. The characteristic parameters for flame-wall extinction for hydrogen in pure oxygen, see Dabireau et al. [11], are quite different from methane, with quenching Peclet number in the range of 1.7. The number of studies with hydrogen is also rather limited in the literature.

To our knowledge, flame-wall interaction studies where the wall is permeable and supplying fuel to the quenching zone are completely missing from the open literature. A new wall boundary condition model is build where the hydrogen flux from the feed side of the membrane reactor is given by the expression above, while further transport and reaction on the permeate side is resolved in detail by the DNS. Even though the present work is limited to 1-D, the model is generally implemented for use in 2-D or 3-D.

2. The DNS modeling approach with the S3D code

The S3D code is a massively parallel three-dimensional DNS code developed by SANDIA National Laboratories [11]. The code solves the compressible Navier-Stokes equations along with equations for species and energy transport coupled with a detailed description of the chemical kinetics. The equations solved and the constitutive relationships (the ideal equation of state, models for reaction rates, molecular transport and thermodynamic properties) are described in detailed in Chen et al. [11]. S3D uses a high-order, non-dissipative numerical scheme, which is an eight-order central differencing scheme in space (third-order at the boundaries) and a six-stage fourth order Runge-Kutta method in time. Spatial filtering

is employed in order to remove any spurious high-frequency noise in the simulations. CHEMKIN and transport libraries are linked to the S3D code to enable detailed evaluation of reaction rates, thermodynamic properties and mixture-averaged transport properties. Characteristic boundary conditions (NSCBC) are used to describe non-reflective (in terms of pressure waves) open boundaries.

In the present work, 1-D direct numerical simulations of premixed laminar hydrogen-air flame propagation and quenching, on both solid and permeable walls, are performed with the S3D code. Thermal diffusion effects, i.e., the Soret effect, have been considered in the simulations. A detailed and accurate description of the chemical kinetics is ensured by incorporating the Li-mechanism [13] with 9 species and 19 elementary reactions. The hydrogen flux through the membrane, F_{H2} (g $cm^{-2}s^{-1}$), is governed by

$$F_{H2}=W_i\, Q/L\, ((P_{f,\,H2})^n-(P_{p,\,H2})^n)\ , \tag{1}$$

where L is the membrane thickness, Q is the hydrogen permeability (mol m-1s-1Pa-n) through the membrane, W_i is the molecular weight, and $P_{f,H2}$ (Pa) is the hydrogen partial pressure where the subscript f and p indicate the feed and permeate side, respectively (see e.g. [7]). The pressure exponent is typically given as n=0.5 for the Palladium membranes considered in the present work. Optimum hydrogen flow rates are ensured by maintaining a large hydrogen partial pressure difference. This can be achieved by introducing hot sweep gases that lowers the partial pressure of hydrogen on the permeate side, or by direct combustion of the hydrogen. In addition, heat supply to the membrane is needed in order to maintain sufficient operating temperature, and to support the endothermic reforming reactions.

In the present work, the partial pressure on the feed side is given as a constant value. The hydrogen flux is further given by the partial pressure difference over the membrane, hence, the flux will vary with the mole fraction of hydrogen on the permeate side in the immediate vicinity of the wall.

The boundary conditions for mass, momentum and pressure are implemented by calculating the gradient of the respective values, and inverting the numerical stencil as described in the following. The mass fraction gradient of hydrogen at the wall is given by the re-arranged Fick's law

$$(\partial Y_i/\partial x)_{x=0}=F_i\,/\,(D_i\,\rho)\ , \tag{2}$$

where Y_i is the mass fraction of species i, (in this case only hydrogen), D_i is the mixture average mass diffusivity and ρ is the fluid density. The species mass fraction at the wall node is further given by inverting the numerical stencil for the mass fraction gradient. Similarly the expression for the pressure gradient at the wall is inverted to give the pressure component at the wall. The pressure gradient is given by re-arranging the momentum equation to

$$(\partial p/\partial x)_{x=0}=-\sum^{Ng}(\partial F_i/\partial t)-(\partial u/\partial x)\sum^{Ng}F_i+(\partial \tau/\partial x)\ , \tag{3}$$

where τ is the stress tensor and u is the wall normal velocity component, and the sums are taken over all gases N_g participating (in this case only hydrogen). The first right hand term in Eq. (3) is neglected in the present work. Finally, the normal velocity component at the wall, u, is given by the mass flux component calculated from Eq. (1).

3. Results

3.1. Case description

A Palladium membrane is taken as the test case for the present computations, with data from Bredesen et al. [5]. The feed side of the membrane is operated at 28.4atm with a partial pressure of hydrogen at 15.2atm. The specific permeability, *Q/L*, is given as 4.0E-07 (mol $m^{-2}s^{-1}Pa^{-0.5}$). The unburned temperature on the permeate side is 773.15K [5], which also is equal to the wall/membrane temperature. The pre-heated stoichiometric mixture of hydrogen and air has an adiabatic flame temperature of 2606K, flame speed of 1224cm/s and flame thickness of 515μm. The domain length is 2cm and is discretized by 2000 nodes. The computations are initialized with a steady state laminar flame profile corresponding to the unburned mixture on the permeate side. The flame front is located 1 cm from the wall at $t=t^0$. This is sufficiently far from the wall in order to avoid initial flame-wall interaction.

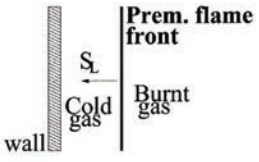

Figure 1 A sketch showing the principle setup of the simulations (from Dabireau et al. [11]). The premixed flame front (at temperature 2606K) is propagating towards the wall, which is maintained at constant temperature (T=773K). For the permeable wall case, a flux of hydrogen is transported through the wall according to equation (1).

3.2. Definitions

The non-dimensional distance to the wall is given by $x^*=x/\delta$, where δ is the undisturbed laminar flame thickness given by $\delta = (T_b-T_u)/\max(|\partial T/\partial x|)$ and T_b and T_u are the burned and unburned gas temperatures, respectively. The non-dimensional time is defined as $t^*=t/t_F$, where t_F is the characteristic residence time given as $t^*= \delta /S_L$, and S_L is the freely propagating laminar flame speed. The non-dimensional temperature is given as $T^* = (T-T_u)/(T_b-T_u)$.

The quenching is defined at the time, t_Q, and location, x_Q, when the reaction rate of fuel starts to decline from its maximum value in the freely propagating flame. When quenching occurs, the flame thickness is reduced to its minimum, δ_Q. The quenching Peclet number is given as the ratio of quenching distance to the quenching flame thickness $Pe_Q=x_Q/\delta_Q$.

3.3. Results and Discussion

For the both cases, the flame initially propagates freely without any disturbance from the wall, before it enters the region where it starts to interact with the wall in terms of heat loss and consumption of the remaining fuel. For the permeable wall case, the flame will enter a near wall region where the premixed reactants are richer than the initial mixture. Note that the amount of additional hydrogen from the permeable wall, accumulated close to the wall, will depend on the time it takes the flame to arrive to the enriched zone. Hence, opposed to the non-permeable case, the solution is dependent on the initial condition and the size of the simulation domain. The hydrogen flux is based on the partial pressure difference between the feed and permeate side of the membrane. Initially, the domain is filled with

premixed hydrogen and air at fixed levels. Figure 2 illustrates the variation of the hydrogen flux through the membrane versus time. The small negative "bump" is caused by a pressure wave that is generated by the marginally incorrect initial condition. As expected, the hydrogen flux is approximately constant (on the present resolution) for the time needed by the flame to reach the wall region and to start consuming the hydrogen fuel in contact with the permeable wall. The reduction in partial pressure of hydrogen near the wall (due to consumption by the flame) induces the increase in hydrogen flux through the membrane until a maximum is reached. After flame extinction the hydrogen is replenished on the permeate side, which in turns reduces the flux through the membrane.

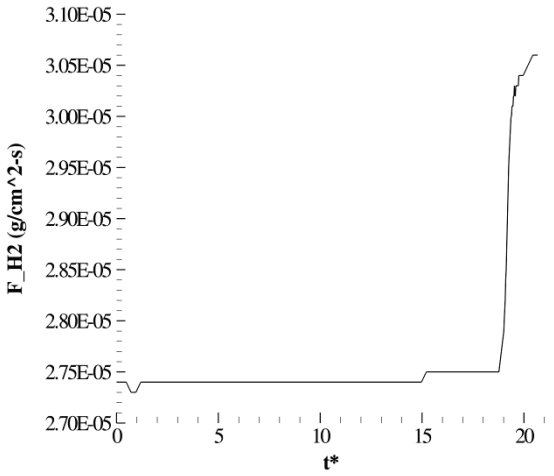

Figure 2 The variation of the hydrogen flux through the membrane versus time

The quenching results are compared for the permeable and the non-permeable wall cases in Table 1. The flame thickness is reduced at quenching for the permeable case compared to the non-permeable case. The temperature profiles from which the quenching flame thickness is calculated are shown in Figure 3 as solid lines. The solid line is taken at the quenching time for both cases, respectively, while the other curves represent about the same absolute time. The maximum temperature gradient which is in inverse proportion to the flame thickness is slightly larger for the permeable than for the non-permeable case. This is the basis for the difference in flame thickness. For hydrogen in general, the freely propagating flame thickness is reduced with increasing equivalence ratio (φ) until about φ=1.7-1.8 where it increases again. Hence, the reduced flame thickness may be due to the enrichment of the mixture close to the wall in the permeable wall case.

Table 1. Comparison of quenching data for the permeable wall and the non-permeable wall cases

	Permeable wall	Non-permeable wall
Quenching Peclet number, Pe_Q	1.015	0.99
Non-dimensional quenching time, $(t^*)_Q$	19.07	19.05
Non-dimensional quenching distance $(x^*)_Q$	0.23	0.27
Flame thickness at quenching δ_Q [μm]	118	141

The quenching distance is also somewhat reduced from the non-permeable to the permeable case. The preferential diffusion of hydrogen increases the transport of hydrogen out from the reaction zone close to the wall. This promotes quenching closer to the wall. For the permeable case, hydrogen is supplied through the wall, which counteracts the reduction of hydrogen fuel in the near wall zone, and, hence, leads to a lower quenching distance. The flux of hydrogen is in this case very small compared to the rather large laminar flame speed. Thus, the difference in quenching time is almost negligible, and the quenching Peclet number is only slightly higher for the permeable wall case. It should also be noted that the timestep on which the simulations are run, which also defines the accuracy in time, is t^*=0.25. Therefore, future simulations should be run with even smaller timestep to achieve higher accuracy in the measurement of quenching time.

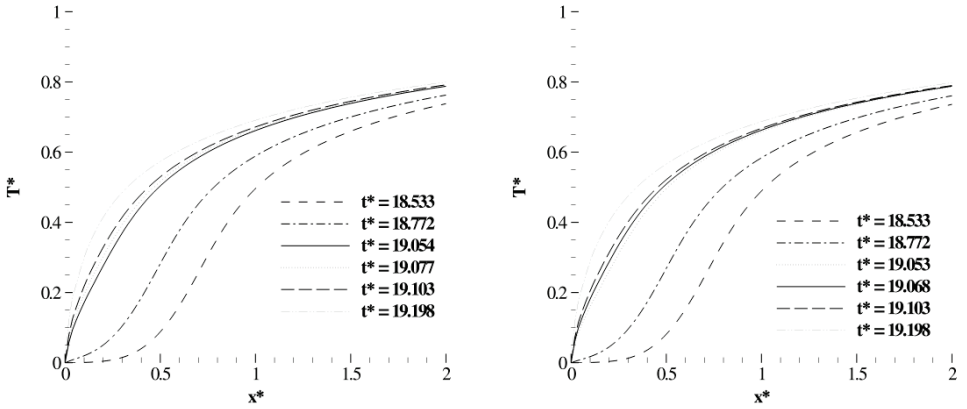

Figure 3 The figures show the non-dimensional temperature as a function of non-dimensional distance from the wall for the non-permeable case (left) and the permeable case (right). The results are given in series as a function of time, where the solid line indicates the time at when quenching occurs.

Due to rather small hydrogen flux, being 2.75E-05 g/(cm^{2}s), the differences between the permeable and the non-permeable cases are very small. According to the literature on membranes the permeability can be increased by almost a factor 100. Larger hydrogen fluxes will be investigated in future work. Combustors are likely to be operated at lean conditions, hence, lean mixtures of hydrogen and air will be investigated in further work. With larger hydrogen fluxes and lean conditions, situations may occur where a hydrogen flame is sustained for a longer time close to the membrane. This is an unwanted situation, since the Palladium membrane can not withstand very high temperatures.

4. Concluding remarks

In this work we consider in principal a membrane reactor with catalytic SMR and/or WSG on the feed side, hydrogen separation and direct combustion of hydrogen on the permeate side, where the ultimate goal is an industrial size novel membrane reactor/combustor concept. The fundamental behavior of quenching towards a permeable wall is compared with a case where the wall is non-permeable. The quenching towards a permeable wall setup has not previously been investigated in the open literature.

A model for the flux of species through a permeable wall (membrane) has been implemented in the DNS code S3D. The results show that the flame thickness at quenching decreases, while the quenching time, the quenching distance, and the Peclet number slightly increases. The present case has a rather limited hydrogen flux which only has a moderate impact on the quenching properties. Further work will involve higher hydrogen fluxes at both lean and rich conditions. Ultimately, the computations will be extended to 3-dimensional cases, for detailed investigations membrane-flame interactions.

Acknowledgements

This publication has been produced with support from the BIGCCS Centre, performed under the Norwegian research program Centres for Environment-friendly Energy Research (FME). The authors acknowledge the following partners for their contributions: Aker Solutions, ConocoPhillips, Det Norske Veritas, Gassco, Hydro, Shell, Statoil, TOTAL, GDF SUEZ and the Research Council of Norway (193816/S60).

References

[1] "A policy strategy for carbon capture and storage", IEA-information paper (2012), url: http://www.iea.org/papers/2012/policy_strategy_for_ccs.pdf
[2] Jordal K, "Benchmarking of power cycles with CO2 capture—The impact of the selected framework" International Journal of Greenhouse Gas Control 2 (2008), 468-77
[3] Foster-Wheeler "Preliminary definition of plants configurations and specifications of membrane operating conditions" Project report in the DEMOYS project (2010) url: http://demoys.rse-web.it/Pubblications/Public-reports.asp
[4] Johannesen E, Jordal, K "Study of a H2 separating membrane reactor for methane steam reforming at conditions relevant for processes with CO2 capture", Energy Conversion and Management 46 (2005) 1059-71
[5] Bredesen, R Jordal, K Bolland, O "High-temperature membranes in power generation with CO2-capture" Chemical Engineering and Processing 43 (2004) 1129-58
[6] Aasen, K Vigeland, B Nordby, T Larring, Y Mejdell, T "Development of a hydrogen membrane reformer based on CO2 emission free gas power plant", GHGT7 (2004) url: http://uregina.ca/ghgt7/PDF/papers/peer/136.pdf
[7] Peters, TA Kaleta, T, Stange, M Bredesen, R "Development of thin binary and terniary PD-based alloy membranes for use in hydrogen production" Journal of Membrane Science 383 (2011) 124-34
[8] Moin, P Mahesh, K "Direct Numerical Simulation: a tool in turbulence research" Annual Review of Fluid Mechanics. 30 (1998), 539–78
[9] Gruber, A Hawkes, ER Sankaran, R Chen, JH "Turbulent flame-wall interaction: a DNS study." Journal of Fluid Mechanics. 658 (2010), 5-32
[10] Egolfopoulos, F.N. Zhang, H. Zhang Z (1997) Wall effects on the propagation and extinction of steady, strained, laminar premixed flames. Combust. Flame 109, 237–252
[11] Dabireau, F Cuenot, B Vermorel, O Poinsot, T (2003) Interaction of flames of H2 CO2 with inert walls. Combust. Flame 135, 123–133

[12] Chen, J.H Choudhary, A De Supinski, B Devries, M Hawkes, E.R Klasky, S Liao, W.K. Ma, K.L Mellor-crummey, J Podhorski, N, Sankaran, R Shende, S Yoo, C (2009) Terascale direct numerical simulations of turbulent combustion using S3D. Comput. Sci. Disc. 2, 1–31

[13] Li, J Zhao, Z Kaxarov, A Dryer, F.L (2004) An updated comprehensive kinetic model of hydrogen combustion. Intl J. Chem. Kinet. 36, 566–575